We are IntechOpen,
the world's leading publisher of
Open Access books
Built by scientists, for scientists

4,800
Open access books available

122,000
International authors and editors

135M
Downloads

Our authors are among the

154
Countries delivered to

TOP 1%
most cited scientists

12.2%
Contributors from top 500 universities

BOOK CITATION INDEX

CLARIVATE ANALYTICS

INDEXED

WEB OF SCIENCE™

Selection of our books indexed in the Book Citation Index
in Web of Science™ Core Collection (BKCI)

Interested in publishing with us?
Contact book.department@intechopen.com

Numbers displayed above are based on latest data collected.
For more information visit www.intechopen.com

Vertex Search Algorithm of Convex Polyhedron Representing Upper Limb Manipulation Ability

Makoto Sasaki[1], Takehiro Iwami[2], Kazuto Miyawaki[3],
Ikuro Sato[4], Goro Obinata[5] and Ashish Dutta[6]
[1]Iwate University,
[2]Akita University,
[3]Akita National College of Technology
[4]Miyagi Cancer Center Research Institute,
[5]Nagoya University
[6]Indian Institute of Technology Kanpur
[1-5]Japan,
[6]India

1. Introduction

In the evaluation of robot manipulator, all possible velocities, accelerations, and forces at the end-effector can be represented as a polyhedra using the concept of manipulability (Yoshikawa, 1990). This evaluation method, which is commonly used in the field of robotics, provides effective knowledge for evaluation of the manipulability of upper and lower limbs considering both the kinematics and dynamics of the system (Sasaki et al., 2008, 2010).

The manipulability of the upper and lower limbs in three-dimensional task space is expressed as an invisible six-dimensional polytope. For such evaluation, a slack variable is generally introduced in order to search for the vertex of the polytope (Shim & Yoon, 1997; Chiacchio et al., 1997; Lee, 2001). However, it is extremely difficult to search for the region of a higher-dimensional polytope accurately using conventional methods because of their huge computational complexity, and it is also difficult to formulate an objective function in the case of linear programming.

In this chapter, we present a manipulating force polytope reflecting an individual's joint torque characteristics as a new evaluation method for assessing the manipulability of an upper limb. We also present a visualization algorithm and a vertex search algorithm for a higher-dimensional polytope based on the geometric characteristic of joint torque space. The effectiveness of the method proposed for quantitative evaluation of the individual's manipulability of the upper limb is confirmed through the presented experimental result.

2. Seven degree of freedom upper-limb model

Figure 1 portrays a seven DOF-rigid-link model of the upper limb. In the model, θ_1, θ_2, and θ_3 represents the shoulder flexion(+)/extension(-), adduction(+)/abduction(-), and external rotation(+)/internal rotation(-) respectively. In addition, θ_4 is elbow flexion(+)/extension(-);

θ_5, θ_6, θ_7 signify wrist supination(+)/pronation(-), palmar flexion(+)/dorsiflexion(-), and radial flexion(+)/ulnar flexion(-) respectively. The physical parameters of each link, e.g., mass, center of gravity, inertia matrix, are calculated using regression equations based on the body weight and link length (Ae et al., 1992). In general, the dynamic equation of motion of the upper limb is given as

$$\boldsymbol{\tau} = M(\boldsymbol{\theta})\ddot{\boldsymbol{\theta}} + h(\boldsymbol{\theta}, \dot{\boldsymbol{\theta}}) + g(\boldsymbol{\theta}) + \boldsymbol{J}^T \boldsymbol{F} , \tag{1}$$

where $\boldsymbol{\tau} \in R^l$ is a joint torque vector, $\boldsymbol{\theta} \in R^l$ is a joint angle vector, $M(\boldsymbol{\theta}) \in R^{l \times l}$ is an inertia matrix, $h(\boldsymbol{\theta}, \dot{\boldsymbol{\theta}}) \in R^l$ are centrifugal and coriolis terms, $g(\boldsymbol{\theta}) \in R^l$ is a gravity term, $\boldsymbol{J} \in R^{n \times l}$ is a Jacobian matrix, $\boldsymbol{F} \in R^n$ is a hand force vector, $l (=7)$ is the number of joints, and $n (\le 6)$ represents the degrees of freedom of the hand force vector. Because the net joint torque for generating the hand force can be written as

$$\tilde{\boldsymbol{\tau}} = \boldsymbol{\tau} - M(\boldsymbol{\theta})\ddot{\boldsymbol{\theta}} - h(\boldsymbol{\theta}, \dot{\boldsymbol{\theta}}) - g(\boldsymbol{\theta}) , \tag{2}$$

the relation between the joint torque and the hand force is given as

$$\tilde{\boldsymbol{\tau}} = \boldsymbol{J}^T \boldsymbol{F} . \tag{3}$$

This equation means that an individual's hand force characteristic is obtained by substituting measurable joint torque characteristics into $\boldsymbol{\tau}$. Because the joint torque characteristics vary according to the joint angle and direction of rotation, the maximum joint torque that can be generated at an arbitrary condition is given as

$$\tilde{\tau}_{imax} = \tau_{imax}(\theta_i) - M_i(\boldsymbol{\theta})\ddot{\boldsymbol{\theta}} - h_i(\boldsymbol{\theta}, \dot{\boldsymbol{\theta}}) - g_i(\boldsymbol{\theta}) \tag{4}$$

$$\tilde{\tau}_{imin} = \tau_{imin}(\theta_i) - M_i(\boldsymbol{\theta})\ddot{\boldsymbol{\theta}} - h_i(\boldsymbol{\theta}, \dot{\boldsymbol{\theta}}) - g_i(\boldsymbol{\theta}) , \tag{5}$$

where $\tau_{imax}(\theta_i)$ and $\tau_{imin}(\theta_i)$ signify the maximum joint torque that can be generated at joint angle θ_i in a positive direction or a negative direction, and $i (=1,2,\cdots,l)$ is the joint number.
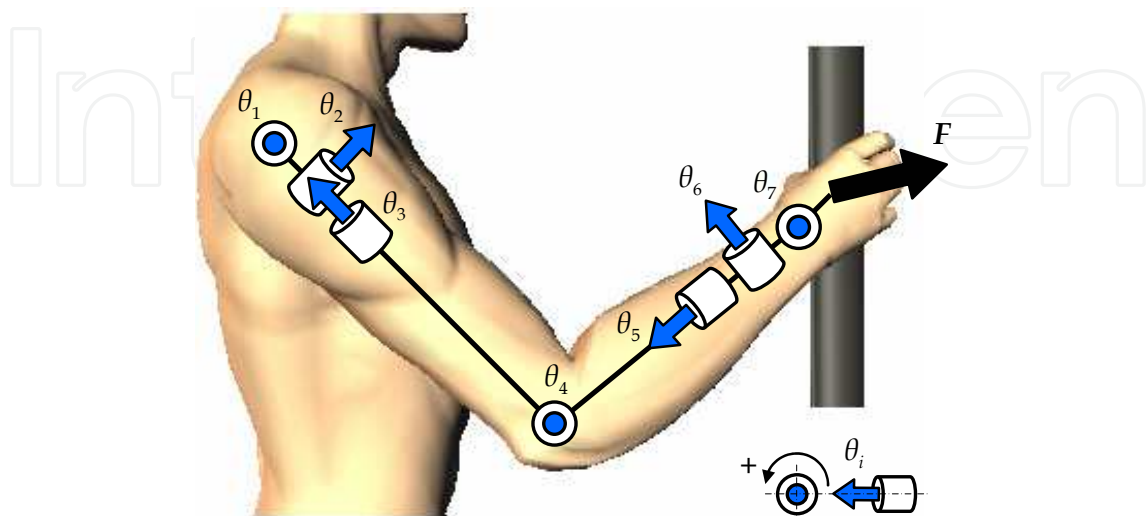

Fig. 1. Seven-rigid-link model of the upper limb.

These joint torques can be quantified using a Cybex (Cybex Inc.) or Biodex machine (Medical Systems Inc.). Therefore, all the possible hand forces encountered during daily life motion is given by the joint torque that satisfies the following conditions.

$$\tilde{\tau}_{imin} \leq \tilde{\tau}_i \leq \tilde{\tau}_{imax} \tag{6}$$

3. Manipulating force polytope considering joint torque characteristics

3.1 Derivation of the polytope

All the hand forces that can be generated during a daily life motion is given by the joint torques satisfying the condition of Eq. (6). The set of all hand forces can be calculated using Eq. (6) and

$$F = (J^T)^{-1}\tilde{\tau} . \tag{7}$$

This set of forces can be expressed as a convex polytope in n-dimensional hand force space. The convex polytope is called the manipulating force polytope. For a redundant manipulator such as the human upper limb $(l > n)$, in general, the set of hand forces cannot be calculated directly because J^T is not a regular matrix. The pseudo-inverse matrix $(J^T)^+$ is a general solution that minimizes the error norm $\|\tilde{\tau} - J^T F\|$ and it is introduced instead of $(J^T)^{-1}$

$$F = (J^T)^+\tilde{\tau} , \tag{8}$$

(Chiacchio et al., 1997). However, Eq. (3) does not always have a solution for hand force because all joint torque space cannot be covered with the range space $R(J^T)$ of J^T, as shown in Fig. 2 (Asada & Slotine, 1986). In other words, a unique solution is not guaranteed and $\tilde{\tau}$ of both sides of the following equation cannot be equated.

$$\tilde{\tau} = J^T F = J^T (J^T)^+ \tilde{\tau} = \tilde{\tau} \tag{9}$$

Therefore, to obtain the manipulating force polytope for a human upper limb, searching the subspace of the joint torque space given by $R(J^T)$ and projecting it to the hand force space is required.

Here, because the null space $N(J)$ of J is an orthogonal complement of $R(J^T)$, the following relation can be written

$$N(J) = \{R(J^T)\}^\perp . \tag{10}$$

In addition, the singular value decomposition of Jacobian matrix J is given as

$$J = U\Sigma V^T = [U_1 \quad U_2]\begin{bmatrix} S & 0 \\ 0 & 0 \end{bmatrix}\begin{bmatrix} V_1^T \\ V_2^T \end{bmatrix}, \tag{11}$$

where $\Sigma \in R^{n \times l}$ is a diagonal matrix with arranged nonzero singular values of J such as $S = \text{diag}(s_1, s_2, \cdots, s_r)$, $U \in R^{n \times n}$ is an orthogonal matrix, $U_1 \in R^{n \times r}$ and $U_2 \in R^{n \times (n-r)}$ are submatrices of U, $V \in R^{l \times l}$ is an orthogonal matrix, $V_1 \in R^{l \times r}$ and $V_2 \in R^{l \times (l-r)}$ are

submatrices of V, and r is the rank of J. Because the column vector v_t $(t=1,2,\cdots,r)$ of V_1 is equal to the base vector of Eq. (10), $R(J^T)$ is represented as the space covered by r base vectors of dimension l. By projecting to the hand force space the joint torque's subspace given by $R(J^T)$, the manipulating force polytope is obtainable.
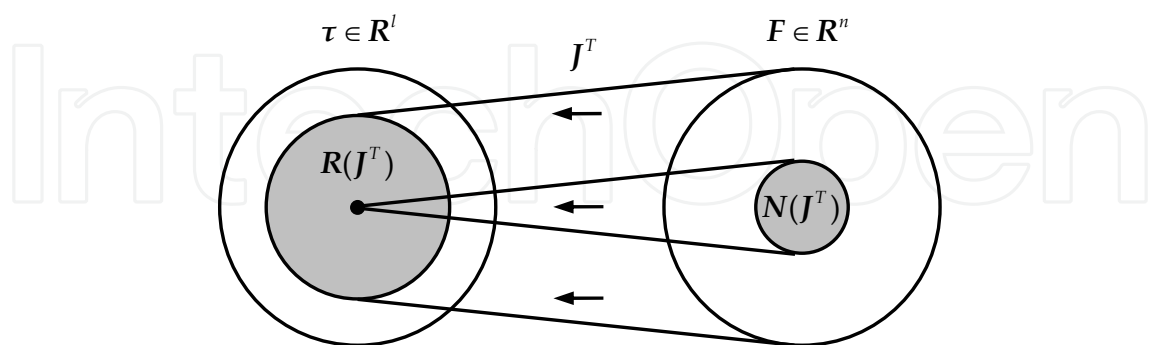

Fig. 2. Null space and range space of J^T.

3.2 Vertex search algorithm for higher dimensional polytope

In order to search for the vertex of the convex polytope, a slack variable is generally introduced. However, the vertex search using a linear programming method such as the simplex method engenders huge computational complexity and a complex definition of the objective function. Especially, it is extremely difficult to search for all vertexes of a high-dimensional polytope. Therefore, we propose a new vertex search algorithm.

The vertex search algorithm is based on the geometric characteristic that the points of intersection between the *l*-dimensional joint torque space and the space covered by r base vectors of dimension l exist in the $(l-r)$-dimensional face of joint torque space. The algorithm is explained using a three-dimensional rectangle in Fig. 3 for clarification.

For $l=3$ and $r=2$, the two-dimensional plane covered by two base vectors intersects with a side (= one dimension) of a three-dimensional rectangle (see Fig. 3(a)). Because its side is a common set of two planes, the number of joint torque components equal to the maximum joint torque $\tilde{\tau}_{imax}$ or the minimum joint torque $\tilde{\tau}_{imin}$ is equal to two. For $l=3$ and $r=1$, the one-dimensional straight line covered by a base vector intersects with a face (= two dimension) of a three-dimensional rectangle (see Fig. 3(b)). The number of joint torque components equal to $\tilde{\tau}_{imax}$ or $\tilde{\tau}_{imin}$ is then equal to one. Consequently, generalizing the geometric characteristics shows that the space covered by r base vectors of dimension l intersects with the $(l-r)$-dimensional face of the *l*-dimensional joint torque space. It also reveals that the number of joint torque components equal to $\tilde{\tau}_{imax}$ or $\tilde{\tau}_{imin}$ is equal to r.

By defining the points of intersection between the *l*-dimensional joint torque space and the range space $R(J^T)$ of J^T is written as

$$K = [k_1, k_2, \cdots, k_r]^T,$$

(12)

the subspace of the joint torque space is given as

$$T = k_1 v_1 + k_2 v_2 + \cdots + k_r v_r = V_1 K.$$

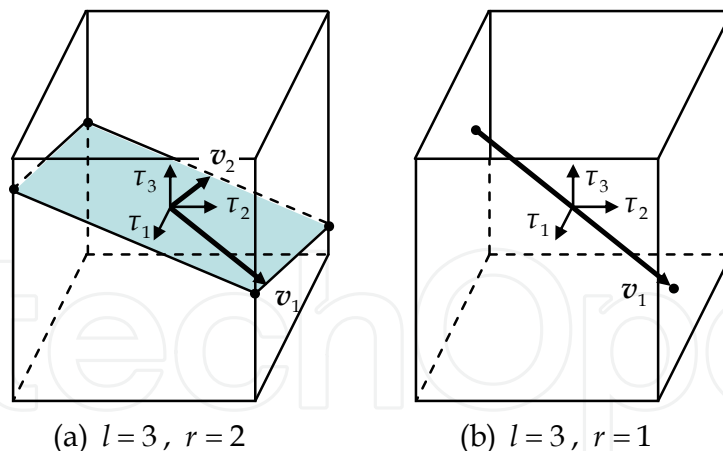(13)

(a) $l = 3$, $r = 2$ (b) $l = 3$, $r = 1$

Fig. 3. Vertexes of l-dimensional convex polytopes.

Equation (13) can also be written as

$$\begin{bmatrix} T_1 \\ T_2 \end{bmatrix} = \begin{bmatrix} \tau_1 \\ \vdots \\ \tau_r \\ \hline \tau_{r+1} \\ \vdots \\ \tau_l \end{bmatrix} = \begin{bmatrix} k_1 v_{11} + k_2 v_{21} + \cdots + k_r v_{r,1} \\ \vdots \\ k_1 v_{1,r} + k_2 v_{2,r} + \cdots + k_r v_{r,r} \\ \hline k_1 v_{1,r+1} + k_2 v_{2,r+1} + \cdots + k_r v_{r,r+1} \\ \vdots \\ k_1 v_{1,l} + k_2 v_{2,l} + \cdots + k_r v_{r,l} \end{bmatrix} = \begin{bmatrix} V_{11} \\ V_{12} \end{bmatrix} K , \tag{14}$$

where $T_1 \in R^r$ and $T_2 \in R^{l-r}$ are submatrices of $T \in R^l$, and where $V_{11} \in R^{r \times r}$ and $V_{12} \in R^{(l-r) \times r}$ are the submatrices of the base vector V_1. From this equation, the relation between T_1 and T_2 is obtained as

$$T_2 = V_{12} K = V_{12} V_{11}^{-1} T_1 . \tag{15}$$

Because there are 'r' joint torque components equal to $\tilde{\tau}_{imax}$ or $\tilde{\tau}_{imin}$ in the intersection points, we can define T_1 as shown below:

$$T_{11} = \begin{bmatrix} \tau_1 \\ \vdots \\ \tau_r \end{bmatrix} = \begin{bmatrix} \tilde{\tau}_{1max} \quad or \quad \tilde{\tau}_{1min} \\ \vdots \\ \tilde{\tau}_{rmax} \quad or \quad \tilde{\tau}_{rmin} \end{bmatrix} \tag{16}$$

The intersection points K are obtained by judging whether the joint torque component of T_2 calculated from Eqs. (15) and (16) satisfies the condition of the joint torque in Eq. (6). Therefore only when T_2 satisfies this condition, the joint torque T is calculated from K,

$$K = V_{11}^{-1} T_1 = V_{12}^{-1} T_2 , \tag{17}$$

And it becomes the vertex of the l-dimensional convex polytope. Herein, the number of combinations which select the n equations from l equations in Eq. (14) and define V_{11} is $_l C_r$, while the number of combinations defining T_1 in Eq. (16) is 2^r. All vertexes of the l dimensional convex polytope can be found by calculating the intersection points in all

combinations. The manipulating force polytope based on human joint torque characteristics is finally expressed by calculating the convex hulls of all the vertexes projected using Eq. (8) on the hand force space. This is done because the vertex of the l-dimensional convex polytope defined by the proposed algorithm always guarantees the unique solution shown in Eq. (9).

3.3 Example

As a simple example of numerical analysis, the three DOF model of the upper limb (three DOF planar redundant manipulator) shown in Fig. 4 is examined. The link lengths L_1, L_2, and L_3 are 0.3, 0.2, and 0.1 m, and joint angles θ_1, θ_2, and θ_3 are 10, 30, and 30 deg, respectively. Maximum joint torques $\tilde{\tau}_{1max}$, $\tilde{\tau}_{1min}$, $\tilde{\tau}_{2max}$, $\tilde{\tau}_{2min}$, $\tilde{\tau}_{3max}$, and $\tilde{\tau}_{3min}$ are 3.5, 3, 2.5, 2, 1.5, and 1 Nm, respectively. Jacobian matrix described in Eq. (6) becomes

$$J = \begin{bmatrix} -L_1 S_1 - L_2 S_{12} - L_3 S_{123} & -L_2 S_{12} - L_3 S_{123} & -L_3 S_{123} \\ L_1 C_1 + L_2 C_{12} + L_3 C_{123} & L_2 C_{12} + L_3 C_{123} & L_3 C_{123} \end{bmatrix}$$
$$= \begin{bmatrix} -0.275 & -0.223 & -0.094 \\ 0.483 & 0.187 & 0.034 \end{bmatrix}. \tag{18}$$

By calculating the singular value decomposition of Jacobian matrix, each matrix U, Σ, and V described in Eq. (11) are obtained as

$$U = \begin{bmatrix} -0.567 & 0.824 \\ 0.824 & 0.567 \end{bmatrix}, \tag{19}$$

$$\Sigma = \begin{bmatrix} 0.626 & 0 & 0 \\ 0 & 0.108 & 0 \end{bmatrix}, \tag{20}$$

$$V = \begin{bmatrix} 0.884 & 0.443 & 0.149 \\ 0.448 & -0.716 & -0.535 \\ 0.130 & -0.540 & 0.832 \end{bmatrix}. \tag{21}$$

All vertexes of the three-dimensional convex polyhedron in joint torque space can be founded using the vertex search algorithm proposed in section 3.2,.

$$\tilde{\tau} = \begin{bmatrix} -3.000 \\ -2.000 \\ -0.750 \end{bmatrix}, \begin{bmatrix} 3.500 \\ 2.500 \\ 0.982 \end{bmatrix}, \begin{bmatrix} -3.000 \\ 1.500 \\ 1.500 \end{bmatrix}, \begin{bmatrix} 3.500 \\ -0.583 \\ -1.000 \end{bmatrix}, \begin{bmatrix} -1.598 \\ -2.000 \\ -1.000 \end{bmatrix}, \begin{bmatrix} 0.598 \\ 2.500 \\ 1.500 \end{bmatrix}. \tag{22}$$

The two-dimensional manipulating force polyhedron is finally expressed by calculating the convex hulls of all the vertexes projected using Eq. (8).

$$F = \begin{bmatrix} 7.207 \\ -2.114 \end{bmatrix}, \begin{bmatrix} -9.846 \\ 1.649 \end{bmatrix}, \begin{bmatrix} -22.981 \\ -19.284 \end{bmatrix}, \begin{bmatrix} 16.747 \\ 16.773 \end{bmatrix}, \begin{bmatrix} 11.901 \\ 3.459 \end{bmatrix}, \begin{bmatrix} -19.561 \\ -9.887 \end{bmatrix}. \tag{23}$$

Figure 5 portrays the 2-dimensional manipulating force polyhedron which presents the set of all possible hand forces.

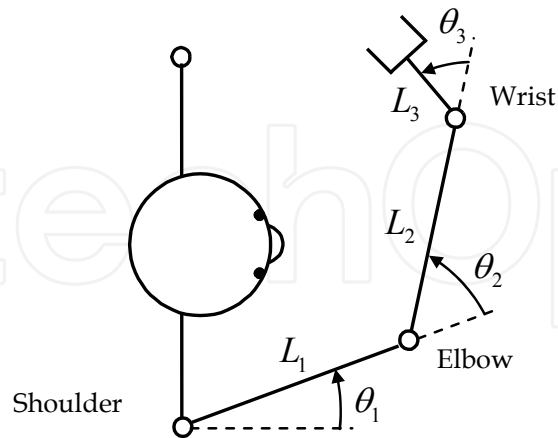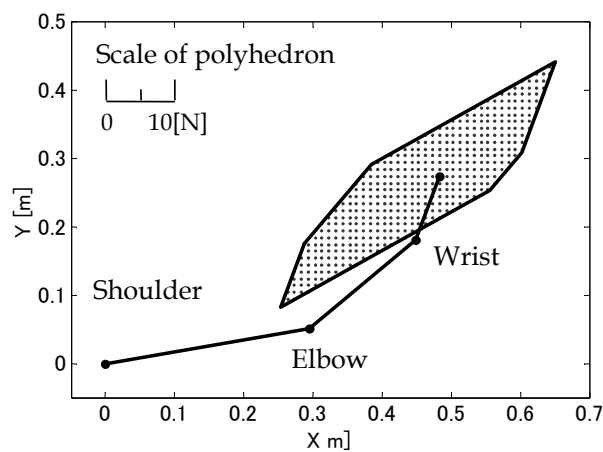

Fig. 4. Three DOF model of the upper limb.

Fig. 5. Two dimensional manipulating force polyhedron.

4. Experimental validation

The proposed evaluation method is verified by comparing the manipulating force polytope based on the maximum joint torque with the measured hand force characteristics
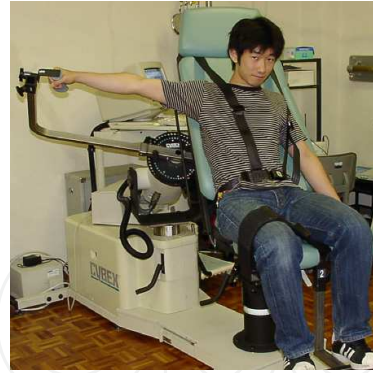
4.1 Measurement of maximum joint torque

In order to calculate the manipulating force polytope reflecting an individual's joint torque characteristics, it is indispensable to measure the maximum joint torque $\tau_{imax}(\theta_i)$ and $\tau_{imin}(\theta_i)$ in advance. For these studies, a Cybex machine (Cybex Inc.) was used for measuring them. The device can measure the maximum joint torque continuously at every joint angle in both the positive and negative directions.

For our experiment, we measured the maximum joint torque produced by the concentric contraction for every pair of movement directions; flexion and extension, adduction and abduction, and external rotation and internal rotation at the shoulder; flexion and extension
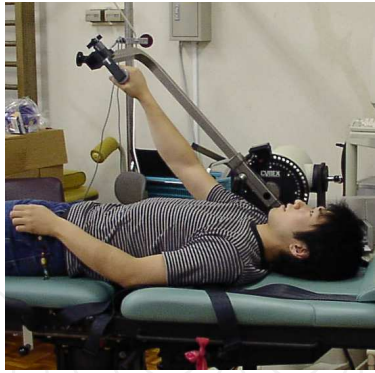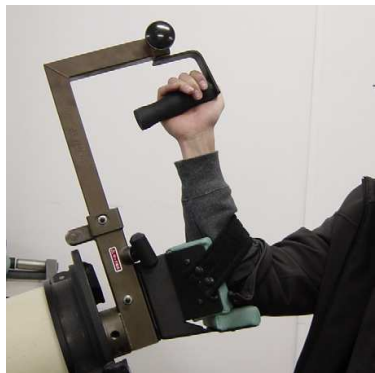
(a) Shoulder flexion/extension   (b) Shoulder adduction/abduction

(c) Shoulder external/internal rotation   (d) Elbow flexion/extension

(e) Wrist supination/pronation   (f) Wrist palmar flexion/dorsiflexion

(g) Wrist radial flexion/ulnar flexion

Fig. 6. Measurement of maximum joint torque.

at the elbow; and supination and pronation, palmar flexion and dorsiflexion, and radial flexion and ulnar flexion at the wrist (see Fig. 6). The participant in the experiment was a person with a spinal cord injury (60 years old, 170 cm, 55 kg, and L2 lumbar injury). The Ethical Committee approved the study protocol, which was fully explained to all subjects in both spoken and written forms, particularly addressing the purpose of the study and the precise procedures to be used and any possible adverse effect.

4.2 Measurement of the hand force and joint angle

Figure 7 shows a measurement system comprising a six-axis force sensor (IFS-105M50A20-I63; Nitta Corp.) and a three-dimensional magnetic position and orientation sensor (Fastrak;Polhemus). The subject added the hand force in eight directions using maximum effort. The hand force applied to the grip was measured using a six-axis force sensor. The receiver to detect the position and posture was put to the hand and the humerus. The joint position and angle of the upper limb, which has 7 degrees of freedom, was calculated using the method developed by Oikawa and Fujita (2000). During this measurement, the subject's upper body was fixed to the back of a chair by belts to eliminate the influence of upper body movements on maximum hand force measurements. The measurements were taken at a sampling frequency of 20 Hz.
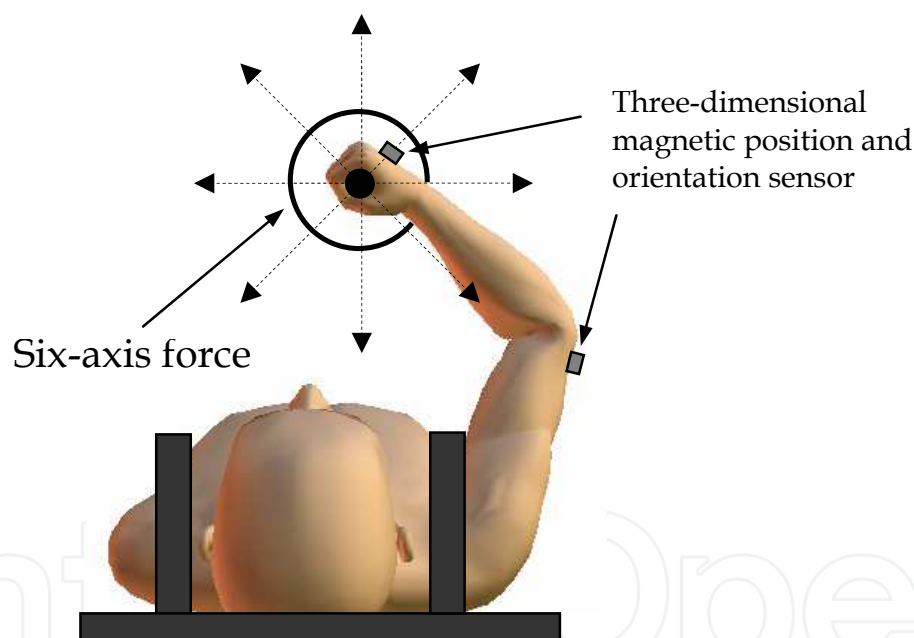

Fig. 7. Measurement system for hand force and upper limb posture.

4.3 Results

Figure 8 depicts a typical example of the maximum joint torque measured using the Cybex device. It is very clear that the ellipsoid described above, which does not consider human joint torque characteristics, is insufficient to evaluate the manipulability of upper limbs because even the joint torque characteristics of healthy person vary greatly according to the joint angle and rotational direction.

Figure 9 portrays the manipulating force polytope, as calculated from the maximum joint torque and posture of the upper limb. The polytope, projected to the two-dimensional plane, represents the set of all the possible hand forces on the horizontal plane, demonstrating a

(a) Shoulder flexion/extension

(b) Shoulder adduction/abduction

(c) Shoulder external/internal rotation

(d) Elbow flexion/extension

(e) Wrist supination/pronation

(f) Wrist palmar flexion/dorsiflexion

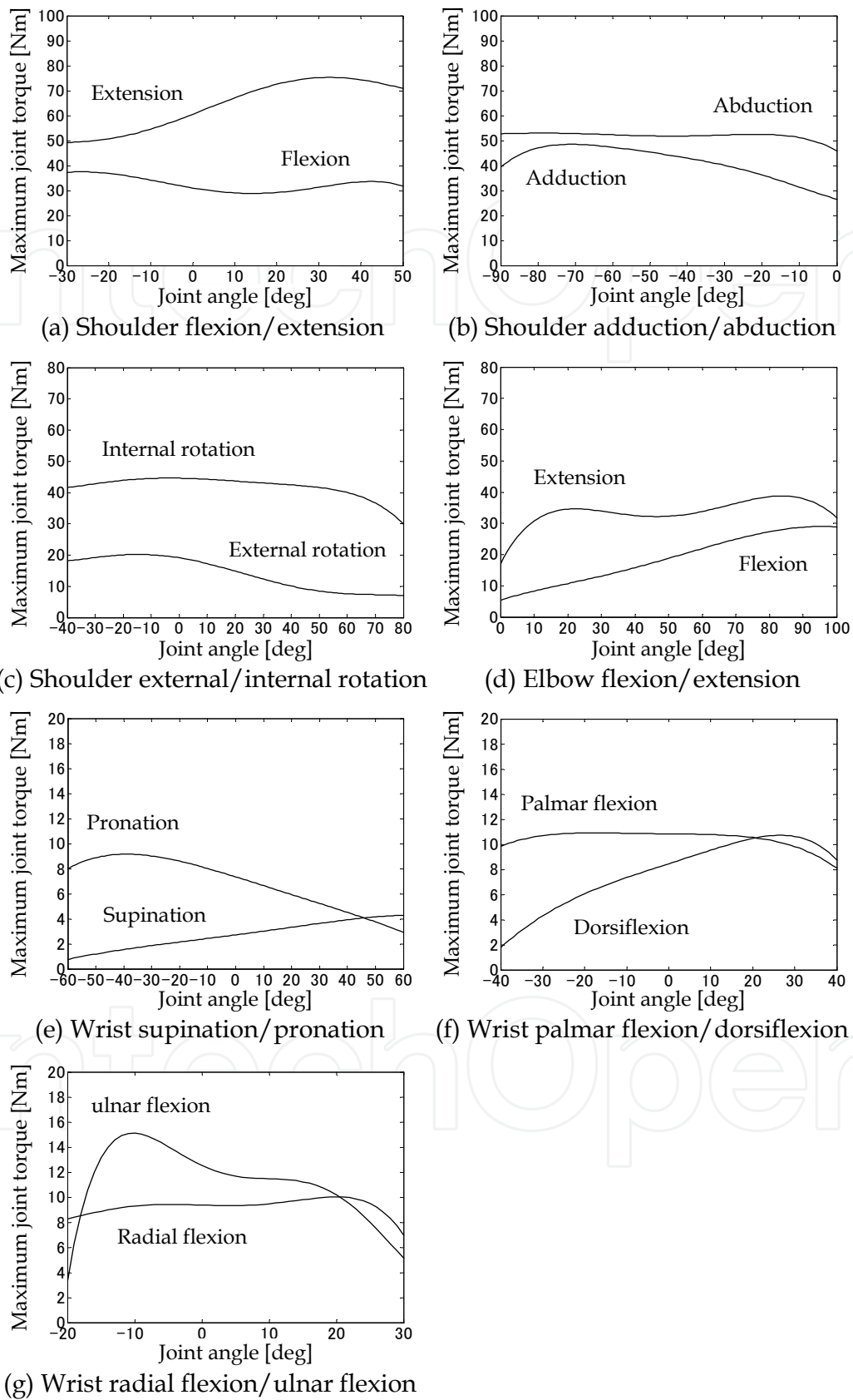(g) Wrist radial flexion/ulnar flexion

Fig. 8. Measurement results of maximum joint torque.

hexagonal shape. This type of shape of the manipulating force polytope agrees with the findings of Oshima et al. (1999) that the distribution of the hand force vector in a two-dimensional plane is a hexagonal shape. In addition, the hand force vector (gray arrow) presumed from the manipulating force polytope approximately corresponds to the measured hand force (black arrow). The effectiveness of the method proposed for quantitative evaluation of an individual's manipulability of the upper limb can be confirmed through the presented experimental result, but it is necessary to perform further verification to achieve a more accurate evaluation.
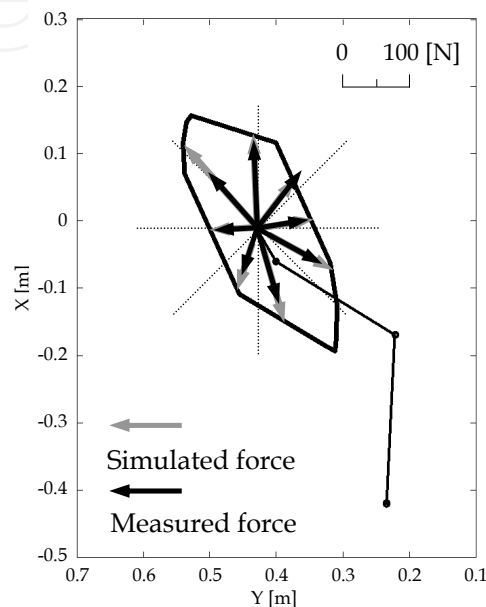
Fig. 9. Manipulating force polytope and hand force.

5. Conclusion

This chapter has presented a manipulating force polytope based on the human joint torque characteristics for evaluation of upper limb manipulability. As described in sections 3, the proposed methods are based on the relation between the joint torque space and the hand force space. Therefore, it is certain that more accurate evaluation can be achieved by expanding these concepts and by considering the relations among muscle space, joint torque space, and hand force space. However, the development of a three-dimensional musculoskeletal model of a human is a respected research area in the field of biomechanics. This is because it is difficult to model an individual's muscle properties strictly, such as the maximum contraction force, the origin, the insertion and the length of each muscle. Also, because of this fact, the proposed evaluation method is a realistic technique by which the influence of the remaining muscle strength or paralysis can be modeled directly and easily as the individual's joint torque characteristics. Nevertheless, further improvements are necessary to achieve a more accurate evaluation because the bi-articular muscle characteristics cannot be accounted sufficiently using the method of separately measuring the maximum joint torque characteristics of each joint.

Through our investigations, we have solved two problems to express the manipulating force polytope based on the measured maximum joint torque. The first is to reflect the human

joint torque characteristics depending on the joint angle and the rotational direction into the formulation of the manipulating force polytope. The second is to derive a new vertex search algorithm for higher-dimensional polytopes to search for all vertexes of convex polytopes without oversight by an easy calculating formula with few computational complexities. It is certain that the proposed methods are effective not only for evaluation of the manipulability of human upper limbs but also for the evaluation of a robot manipulator's manipulation capability because no reports, even in the robotics literature, have described solutions to these problems. Therefore, the proposed methods can probably contribute to progress in the field of robotics in a big way, offering useful new findings.

6. Acknowledgements

7. References

Ae, M.; Tang, H.P. & Yokoi, T. (1992). Estimation of inertia properties of the body segments in Japanese athletes, In: *Biomechanism*, Vol. 11, pp. 23–32, The Society of Biomechanisms Japan, ISBN 978-4-13-060132-0.

Asada, H. & Slotine, J.-J.E. (1986). *Robot Analysis and Control*, John Wiley and Sons, ISBN 0-471-83029-1.

Chiacchio, P.; Bouffard-Vercelli, Y. & Pierrot, F. (1997). Force polytope and force ellipsoid for redundant manipulators. *Journal of Robotic Systems*, Vol. 14, No. 8, pp. 613–620, ISSN 0741-2223.

Lee, J. (2001). A structured algorithm for minimum l∞-norm solutions and its application to a robot velocity workspace analysis. *Robotica*, Vol. 19, pp. 343–352, ISSN 0263-5747.

Oikawa, K. & Fujita K. (2000). Algorithm for calculating seven joint angles of upper extremity from positions and Euler angles of upper arm and hand. *Journal of the Society of Biomechanisms*, Vol. 24, No. 1, pp. 53–60, ISSN 0285-0885.

Oshima, T.; Fujikawa, T. & Kumamoto, M. (1999). Functional evaluation of effective muscle strength based on a muscle coordinate system consisted of bi-articular and mono-articular muscles: contractile forces and output forces of human limbs. *Journal of the Japan Society for Precision Engineering*, Vol. 65, No. 12, pp. 1772–1777, ISSN 0912-0289.

Sasaki, M.; Kimura, T.; Matsuo, K.; Obinata, G.; Iwami, T.; Miyawaki, K. & Kiguchi, K. (2008). Simulator for optimal wheelchair design. *Journal of Robotics and Mechatronics*, Vol. 20, No. 6, pp. 854–862, ISSN 0915-3942.

Sasaki, M.; Iwami, T.; Miyawaki, K.; Sato, I.; Obinata, G. & Dutta, A. (2010). Higher dimensional spatial expression of upper limb manipulation ability based on human joint torque characteristics. *Robot Manipulators, New Achievements*, INTECH, pp.693-718, ISBN 978-953-307-090-2.

Shim, I.C. & Yoon, Y.S. (1997). Stabilization constraint method for torque optimization of a redundant manipulator, *Proceedings of the 1997 IEEE International Conference on Robotics and Automation*, pp. 2403–2408, ISBN 0-7803-3612-7, Albuquerque, NM, April, 1997.

Yoshikawa, T. (1990). *Foundations of Robotics: Analysis and Control*, MIT Press, ISBN 0-262-24028-9.
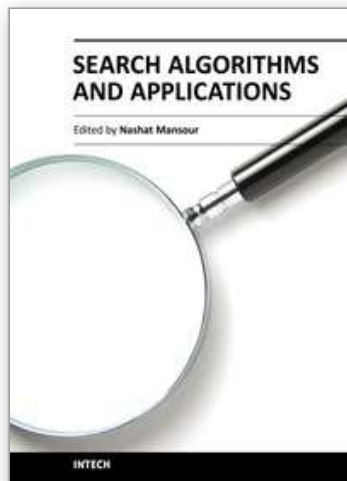
Search Algorithms and Applications

Edited by Prof. Nashat Mansour

Search algorithms aim to find solutions or objects with specified properties and constraints in a large solution search space or among a collection of objects. A solution can be a set of value assignments to variables that will satisfy the constraints or a sub-structure of a given discrete structure. In addition, there are search algorithms, mostly probabilistic, that are designed for the prospective quantum computer. This book demonstrates the wide applicability of search algorithms for the purpose of developing useful and practical solutions to problems that arise in a variety of problem domains. Although it is targeted to a wide group of readers: researchers, graduate students, and practitioners, it does not offer an exhaustive coverage of search algorithms and applications. The chapters are organized into three parts: Population-based and quantum search algorithms, Search algorithms for image and video processing, and Search algorithms for engineering applications.

INTECH
open science | open minds